Topotecan and Irinotecan as potential inhibitors of PARP-1

Yueyi Bao[1], Yizhou Yu[2, *]

[1] The Hill School, Beech Street, Pottstown, PA, U.S.A

[2] MRC Toxicology Unit, University of Cambridge, Tennis Court Road, Cambridge, U.K.

* Corresponding Author Email: yizhou0421@gmail.com

Abstract. Alzheimer's disease (AD) is the most prevalent neurodegenerative disease worldwide, but disease-modifying treatments are still lacking. Poly (ADP-ribose) polymerases (PARPs) consume nicotinamide adenine dinucleotide (NAD) to repair DNA. Excessive PARP activation can deplete NAD in neurons, contributing to mitochondrial dysfunction and cell death. Mutations in the *PARP-1* gene leading to lower PARP-1 levels are protective in AD. This suggests that molecular inhibitors of PARP-1 could have therapeutic potential for AD. Here, we trained a machine learning model to predict potential inhibitors of PARP-1 from FDA-approved drugs. First, we generated multimodal molecular descriptors and trained a random forest regression model. We then performed in silico screening on over 1000 compounds and generated their IC50 on PARP-1. The predicted top 3 most potent predicted inhibitors were Bryamycin, Topotecan, and Irinotecan. Bryamycin is a peptide while Topotecan and Irinotecan are small molecules. To further characterize the binding conformations of these small molecules, we performed molecular modeling to determine the binding poses and energy of Topotecan and Irinotecan. Our *in silico* docking results showed that Topotecan is a more potent inhibitor of PARP-1 than Irinotecan. We then analyzed the differential gene expression in the brain upon Topotecan treatment and found putative neuroprotective pathways. We conclude that Topotecan could be a potential therapeutic method against neurodegeneration through PARP-1 inhibition. Future studies are required to reveal the biochemical effect of Topotecan on PARP-1 activity and the therapeutic potential of Topotecan in animal models of AD.

Keywords: Alzheimer's Disease; Poly [ADP-ribose] polymerase 1; Topotecan; Nicotinamide adenine dinucleotide; Random Forest Regressor; Molecular Docking; Gene Expression Analysis.

1. Introduction

Alzheimer's disease (AD) is the most common neurodegenerative disease worldwide with an increasing prevalence in the aging population. It is considered to be one of the principal causes of age-related dementia. AD patients have severe cognitive impairment as well as language and memory deficits. The hallmarks of AD pathology are marked by the accumulation of extracellular amyloid-β plaques in the brain followed by intracellular neurofibrillary tangle growth (Huber et al., 2017). The amyloid-β plaques are fragments of the amyloid peptide precursor protein. The main component of neurofibrillary tangles is the cytoskeleton protein known as the tau protein, in a hyperphosphorylated form (Hernández et al., 2010). Together, these two neurotoxic proteins trigger a cascade of molecular events including DNA damage, eventually leading to mitochondrial dysfunction and cell death (Houten et al., 2016).

Based on the research around these two proteins, several interventions were proposed to modulate the hallmarks of AD. In this regard, nicotinamide adenine dinucleotide (NAD) is a universal intracellular electron transporter that plays a central role in most of the processes of neurodegeneration (Hou et al., 2019). Importantly, NAD is a substrate in several important reactions such as DNA repair, the maintenance of intracellular calcium homeostasis, and mitochondrial bioenergetics (Berger et al., 2004).

When severe cell injury like intense DNA oxidative damage happens, Poly [ADP-ribose] polymerase 1 (PARP-1) will be activated (Wang et al., 2011; Fatokun et al., 2014; Dawson and Dawson, 2017). Upon DNA damage, PARP-1 adds an ADP-ribose to itself, leading to a 500-fold increase in its activity and recruiting other proteins in DNA repair pathways (Benjamin & Gill, 1980). In pathological situations, PARP-1 hyperactivation consumes large amounts of cellular NAD+ and

ATP, which in turn activates the release of apoptosis-inducing factors from mitochondria that translocates to the nucleus, producing chromatin condensation and large-scale DNA fragmentation (Wang et al., 2011). Once activated, this DNA repair mechanism could result in Parthanatos, a type of programmed cell death (Dawson and Dawson, 2017). This type of death is observed in different cells of the organism, including neurons (Lee et al., 2013), and is present in neurodegenerative disorders such as Parkinson's disease and AD (Langston et al., 1983; Fatokun et al., 2014). These findings strongly support the idea that PARP-1 plays a key role in Parthanatos, mitochondrial function, and inflammation that occurs in AD (Salech et al., 2020).

There are a series of experimental and clinical studies supporting the role of PARP-1 inhibition as a potential adjunctive therapeutic method for AD. PARP-1 inhibitors deserve further research in this field (Salech et al., 2020). Importantly, PARP-1 inhibitors have been developed for other diseases like cancer. Small molecular inhibitors have gradually gained acceptance as therapies for degenerative diseases (Megino-Luque et al., 2020). However, the use of these inhibitors for early AD treatment needs to be further explored. While FDA-approved PARP-1 inhibitors including olaparib, rucaparib, talazoparib, and niraparib are used for cancer treatment, they have several off-target toxic effects (Antolín & Mestres, 2014). Specifically, these canonical PARP-1 inhibitors have been shown to inhibit various kinases (Antolin et al., 2020). Kinases are a type of protein that activates or inhibits a protein by adding a phosphate group. Kinases are dysregulated in AD, and the off-target properties of currently used PARP-1 inhibitors could potentially be dangerous for AD patients (Morshed et al., 2021). There is therefore a need of identifying novel PARP-1 inhibitors to treat neurodegenerative diseases. Additionally, kinases are also dysregulated in some cancer patients (Hijazi et al., 2020), indicating that novel PARP-1 inhibitors will less off-target effects could be useful for cancer patients who would benefit from PARP-1 inhibitors with less kinase toxicity.

Here, we trained a machine learning model to predict the potential of FDA-approved drugs for inhibiting PARP-1. First, we gathered drug data from PubChem and processed the data by generating molecular descriptors, molecular sentences, and molecular fingerprints. We established our model based on the Random Forest Regressor, which generates different regression trees for the final prediction. We then performed *in silico* docking to analyze the binding conformation of the predicted compounds. We reasoned that our model could be an efficient way to predict a drug's ability in inhibiting PARP-1 protein. We believe that drugs with low IC50 values deserve further investigation to explore their impacts on PARP-1 inhibition.

2. Method

2.1. Workflow and data collection

In this project, we aim to combine bioinformatics and in vitro methods to identify PARP-1 inhibitors. First, we extracted data on the molecular inhibitors of the human PARP-1 protein from PubChem. In order to build a regression model, we kept the PARP-1 inhibitors that contain an IC50 value, which is the concentration of a drug needed to inhibit the activity of PARP-1 by 50%. We chose IC50 instead of other activity types as the value of IC50 correlates inversely with the potency of drugs, and was the most thoroughly annotated feature. We calculated the natural logarithm of the IC50 values to have a normally distributed dataset.

2.2. Generation of molecular features

Then, we generated molecular descriptors for each drug. To acquire a comprehensive set of features for each molecule, we combined basic molecular information, vector representations, and molecular fingerprints into 2D and 3D representations.

2.2.1. Basic representations

We first quantified the number of C, N, O, and Cl atoms, as well as other molecular descriptors including the number of atoms, number of heavy atoms, molecular weight, number of valence electrons, and the topological surface area of the molecule.

2.2.2. Molecular fingerprints

We computed molecular fingerprints for each molecule. Molecular fingerprints are a way of encoding the structure of a molecule. It consists of a series of binary digits that represent the presence or absence of particular substructures in the molecule. We decided to use 2048 binary digits with a radius of two, using RDkit.

2.2.3. Representation of molecules as sentences

In order to make the predictive model more accurate, we generated features using Mol2Vec, an unsupervised machine approach to learning vector representations of molecular substructures (Jaeger et al., 2018). The model followed a natural language processing strategy and considers molecules as sentences and substructures as words. The introduction of Mol2Vec helped to increase the accuracy of the model, but we decided to keep modifying the model for the sake of higher accuracy.

2.2.4 Multidimensional representations

In order to add information on higher dimensional information, we imported another model called Mordred. Mordred is a previously developed application that can calculate more than 1800 two- and three-dimensional descriptors (Moriwaki et al., 2018). We obtained 1613 additional molecular descriptors by using Mordred.

2.3. Principal component analysis for the training set

Before training the model, we performed Principal Component Analysis (PCA) to the training dataset, which simplifies the complexity of high-dimensional data while retaining trends and patterns (Lever et al., 2017). Since we have over 4000 features for each molecule, the possibility of an increased error rate due to the correlation or association within the features cannot be overlooked. The results of the PCA for the top 2 components showed that the data is far from being near a 2-dimensional subspace.

2.4. Model training and optimization

After generating molecular features, we made several attempts at training the model with different algorithms, including a random forest regressor, a linear regressor, and a ridge regressor. By comparing and contrasting the accuracy of the results and their efficiency, we decided to build our model using the random forest regressor instead of the linear regressor or the ridge regressor.

First introduced by Breiman in 2001, random forests are a collection of regression trees that use binary splits to determine outcome predictions. Moreover, the random forests regressor is capable of generating different regression trees that compare data based on different standards. The model will then average the results from the different trees to conclude a final model. We decided to use this regressor due to its ability to eliminate potential errors due to the linearity in the dataset.

After the model is trained and tested on Google Colab, we saved and exported the machine learning model as a package to make it accessible and user-friendly. In order to achieve this goal, we decided to use the pickle module. The pickle module implements a fundamental, but powerful algorithm for serializing and de-serializing a Python object structure, which in our case, is the random forest regression model (*Saving a Machine Learning Model*, 2018). After this step, we obtain the model that receives 3429 features of a single molecule to predict its IC50 value with PARP-1 protein.

Then, we used the data from Prestwick Chemical Library to test the model, and obtain the top three drugs with the lowest IC50 value, which are the most effective inhibitors of PARP-1.

2.5. Molecular docking

Docking simulations of the top three drugs within the ligand binding domain of PARP-1 protein were performed using AutoDock Vina, an open-source program for doing molecular docking. Before doing the docking, we downloaded the 3D structures of PARP-1 protein from the Protein Data Bank (ID: 7S6H and 7S6M) and the drugs from *PubChem*. We added charges to both the receptor (PARP-1) and the potential inhibitors to be tested and converted them into .pdtqt files. We calculated the location of the search, the search center, and the area of the search box based on the location of the original bounding ligand. After all the preparation works were done, we performed the docking using an "exhaustiveness" value of 300 and selected the conformation with the lowest binding energy for analysis. Images and analyses were performed using PyMol. Specifically, we identified the potential interactors as the amino acid residues of PARP-1 within 4 angstroms of the bound drug. From these residues, we found all the polar contacts between the PARP-1 protein and the drug.

2.6. Gene expression analysis

The analysis of gene expression of mice with breast cancer treated with topotecan is done with Differential Expression Analysis for Sequence (DESeq), a software that estimates variance-mean dependence in count data from high-throughput sequencing assays and tests for differential expression based on a model using the negative binomial distribution (Anders et al., 2016). We separated the genes by the positivity of their log fold change in order to investigate the function influenced by the treatment of Topotecan.

Then, we utilized STRING, an online platform for Protein-Protein Interaction Networks Functional Enrichment Analysis to analyze the different pathways involved in the increased and decreased groups (*STRING: Functional Protein Association Networks*, n.d.). Using STRING, we found the function that increased and decreased the most according to the strength of UniProt pathways and analyzed the function of genes involved in these functions.

3. Result

3.1. AI-aided generation of molecular features for model training

PARP-1 overactivation is linked to mitochondrial dysfunction in neurodegenerative diseases, and its inhibition could be a potential therapeutic method (Figure 1A). To develop a machine learning model to predict inhibitors of PARP-1, we queried the PubChem database for information on the molecules containing information on PARP-1 (Figure 1B). Out of the 5884 possible known molecular interactors, we filtered out the molecules that do not have specific IC50 values for the PARP-1 protein. This resulted in 2410 molecules. We then generated multidimensional features of these molecules (Figure 1C). Specifically, we generated 1D information using molecular fingerprints, which are binary digits that represent the presence or not of a substructure. Using Mol2Vec, we then represented molecules as sentences, which captures the general structural information of the molecule. Finally, we captured 2D and 3D quantitative structure-property relationship data of these molecules using Mordred (Moriwaki et al., 2018). A principal component projection of the training dataset, based on the generated molecular features is shown (Figure 1D).

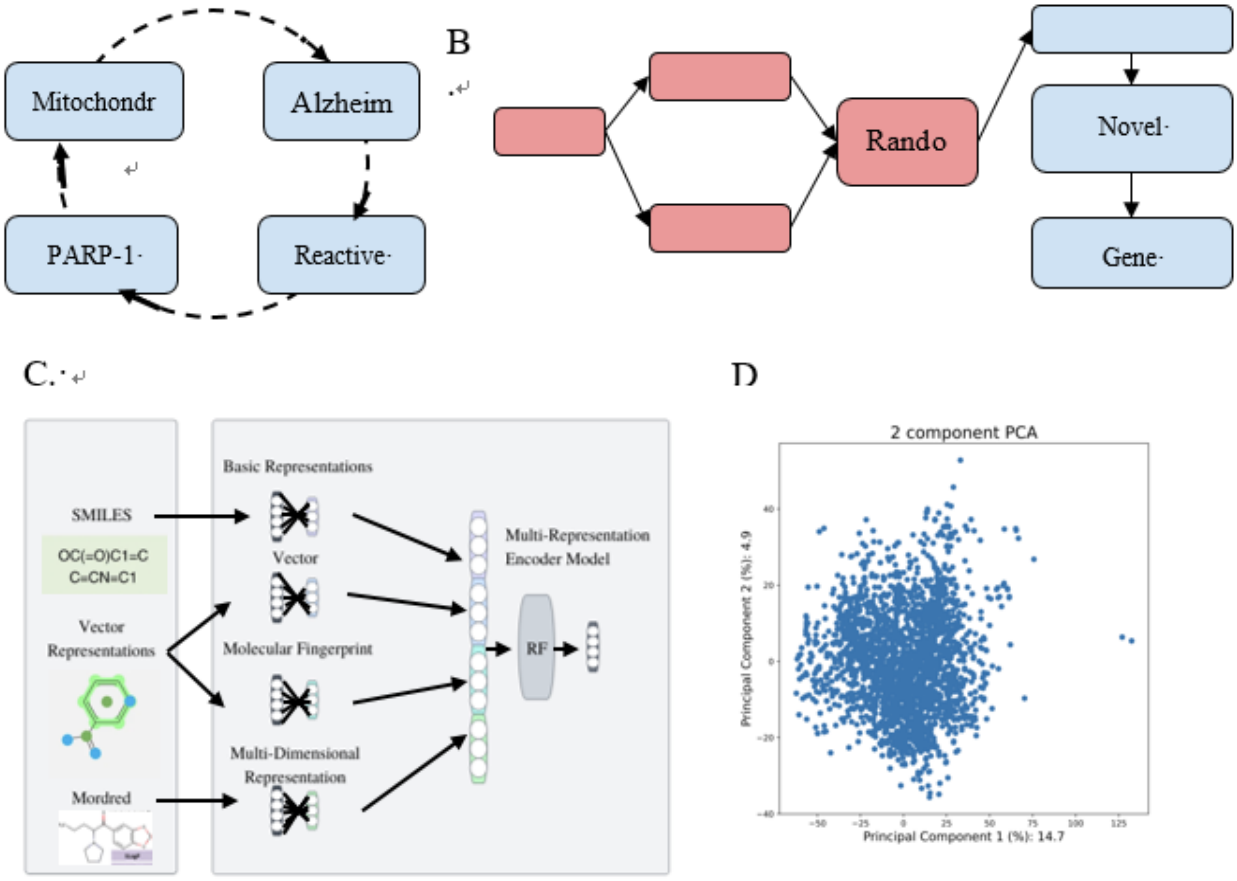

Figure 1. Workflow and rationale.

A. Hallmarks of Alzheimer's disease such as amyloid-β or neurofibrillary tangles cause neurons to accumulate reactive oxygen species (ROS). ROS in turn causes DNA damage, which triggers PARP-1 to repair DNA. PARP-1 overactivation depletes neurons from NAD, leading to mitochondrial dysfunction and further exacerbating Alzheimer's disease pathology.

B. Workflow of the analysis. The first step of the analysis is to perform molecular screening using machine learning (in red) and the second step is to analyze the binding mechanisms of the predicted drugs on PARP-1 (in blue).

C. Feature generation workflow. See Generation of molecular features in the Methods section for more information.

D. Projection of the training dataset.

3.2. Model training and prediction of PARP-1 inhibitors

Next, we aimed to build a model to predict novel inhibitors of PARP-1 in a list of FDA-approved drugs. Drug repurposing refers to the identification of novel therapeutic properties from existing FDA-approved drugs. This strategy is more efficient than developing new drugs for inhibiting PARP-1 since FDA-approved drugs contain multiple known molecular properties and side effects. Before applying the model obtained to the Prestwick Chemical Library, we applied a principal component projection of the training and testing dataset, based on the generated molecular features for both data sets (Figure 2A). The first principal component accounting for 23.2% of the variance indicates that both the training set of our model and the prediction set from Prestwick are similar. However, the second principal component highlights some heterogeneity between these datasets, indicating that the data on which our model is trained is slightly different than the dataset that our model will be used to predict.

After training a random forest regressor, we applied the model to the training data to test it s accuracy. A graph of the actual and predicted value of IC50 value for each drug is shown

(Figure 2B). The model yielded a mean squared error of 2.41 and a mean absolute error of 1. 13, which is equivalent to an IC50 value of 11.13 and 3.10 respectively. We deemed this error to be acceptable since the maximal IC50 is 4200 and the minimal IC50 is $2x10^{-5}$. Applying t he model to the Prestwick testing data, we obtained the IC50 value for each molecule and ran ked them from least to greatest. The ranked chart showed the top 3 PARP-1 inhibitors we obta ined through the model (Figure 2C). These are Bryamycin, Topotecan, and Irinotecan. Bryamy cin is an antimicrobial peptide whereas Topotecan and Irinotecan are small molecule inhibitors of DNA Topoisomerase. Since our model was trained on a dataset of small molecules, we foc used on Topotecan and Irinotecan. To understand how the molecular predictions were generate d, we sought to analyze drugs in our training set that are most similar to the predicted inhibito rs. Using the nearest neighbor function based on principal components, we found that 15-acetyl -9,19-diazapentacyclo[10.7.0.02,6.07,11.013,18]nonadeca-1(12),2(6),7(11),13(18),14,16-hexaene-8, 10-dione (PubChem CID 9944838) and *N*-methyl-8-oxo-*N*-(pyridin-2-ylmethyl)-9,19-diazapentac yclo[10.7.0.02,6.07,11.013,18]nonadeca-1(12),2(6),7(11),13(18),14,16-hexaene-15-carboxamide (P ubChem CID 44408203) are similar to Topotecan and Irinotecan respectively (Figure 2D). Bas ed on their similarities, we reason that there could be shared inhibitory mechanisms. The comp ound 9944838 has an experimental value against PARP1 of 17nM and the predicted IC50 valu e of Topotecan is larger, at around 70nM. Contrastingly, the IC 50 value of compound 444082 03 is 237 nM and that of its predicted neighbor is 76.11 nM, indicating that Irinotecan is a str onger PARP1 inhibitor than compound 44408203. Importantly, these molecules have been sho wn to improve NAD+ levels in yeast, suggesting that these might be a possible option to incre ase NAD+ levels in the AD context.

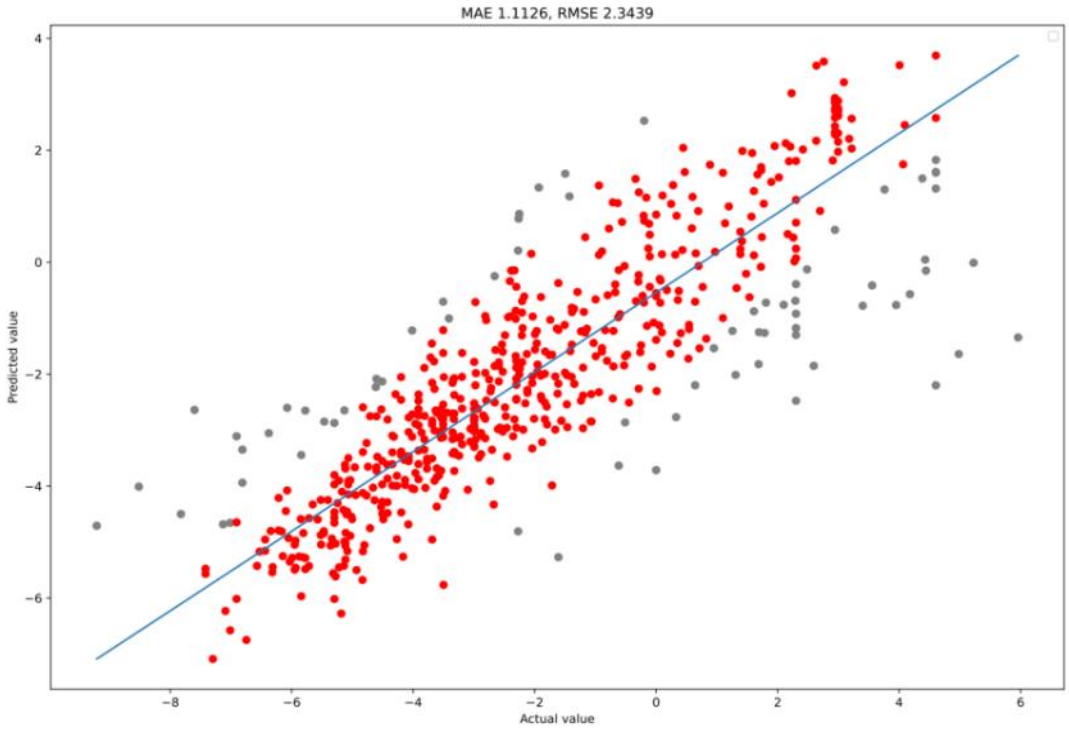

Figure 2. Bryamycin, Topotecan, and Irinotecan are potential inhibitors of the PARP-1 protein.

A. Representation of data from both training and testing sets. The data from the training set is colored in blue while the data from Prestwick Chemical Library is colored in green.

B. Accuracy of the random forest regressor. Our model resulted in a root mean squared value of 2.41, which is equivalent to an IC50 value of 11.13. The grey dots are prediction values with errors larger than or equal to the root mean squared error.

C. Top 3 predicted PARP-1 inhibitors from the Prestwick library with their predicted IC50 values in nM.

D. Molecular structure of Topotecan (1) and 15-acetyl-9,19-diazapentacyclo[10.7.0.02,6.07,11.013,18]nonadeca-1(12),2(6),7(11),13(18),14,16-hexaene-8,10-dione (PubChem CID 9944838) (2) Molecular structure of Irinotecan (i) and *N*-methyl-8-oxo-*N*-(pyridin-2-ylmethyl)-9,19-diazapentacyclo[10.7.0.02,6.07,11.013,18]nonadeca-1(12),2(6),7(11),13(18),14,16-hexaene-15-carboxamide (PubChem CID 44408203) (ii)

3.3. Molecular modeling of the predicted inhibitors Topotecan and Irinotecan binding to PARP-1

In order to assess the molecular and atomic interactions between the predicted novel PARP-1 inhibitors and their protein target, we used molecular docking to understand how these molecules might inhibit PARP-1. We identified the top three drugs and focused on the second and third top inhibitors (Topotecan and Irinotecan) as they are small molecules. We used to AutoDock Vina to investigate the docking position and energy for drug 2 and drug 3 on the human PARP-1 protein. The general docking of the original ligand, Topotecan, and Irinotecan are shown (Figure 3A). Negative binding energy in Autodock Vina indicates a stronger binding potential.

To analyze the drug-protein interactions, we selected the amino acids in PARP-1 protein within 4 Angstroms of any atom from the current ligand. First, we determined the docking position of the original ligand (2-[4-[(2S,3S,4R,5R)-5-(6-aminopurin-9-yl)-3,4-bis(oxidanyl)oxolan-2-yl]carbonylpiperazin-1-yl]-N-(1-oxidanylidene-2,3-dihydroisoindol-4-yl)ethanamide) on the PARP-1 protein (Figure 3B). Then, we obtained the docking position for Topotecan, which cost -12.474 kcal/mol (Figure 3C). We repeated our steps with Irinotecan, whose energy cost is slightly higher than Topotecan with -11.157 kcal/mol (Figure 3D). Interestingly, the binding energy of Topotecan is even lower than that of the original ligand, suggesting that Topotecan has more inhibitory potential than the known inhibitor if it reaches the binding site. The binding energy of Irinotecan is higher than that of the original ligand, but still very low. These results indicate that both Topotecan and Irinotecan could theoretically bind strongly to the NAD+ site of PARP-1 if they reach that site. Since Topotecan has a higher affinity than the original ligand, there is more potential for Topotecan to inhibit PARP1.

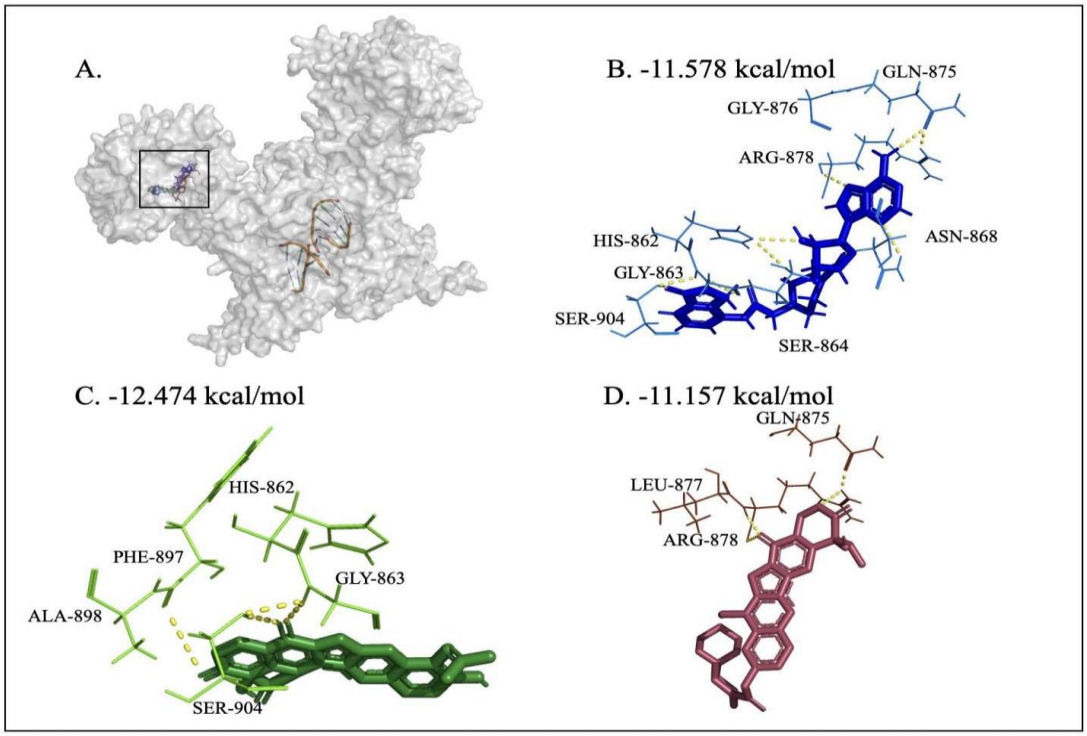

Figure 3. Binding conformations of the predicted PARP-1 inhibitors.

A. Overall structure of PARP-1 (PDB ID: 7S6H) Topotecan and Irinotecan at low magnification. The protein is indicated in grey and the DNA bound to PARP is in orange. The box represents the docked area.

B-D. Docking of original ligand (B), Topotecan (C) and Irinotecan (D). The ligands are represented as sticks whereas the amino acids are represented as lines. The polar contacts are in yellow dashed lines. The name of the original crystalised ligand is: 2-[4-[(2S,3S,4R,5R)-5-(6-aminopurin-9-yl)-3,4-bis(oxidanyl)oxolan-2-yl]carbonylpiperazin-1-yl]-N-(1-oxidanylidene-2,3-dihydroisoindol-4-yl)ethanamide.

Since previous studies have shown that Topotecan and Irinotecan could bind to the DNA-protein interface of DNA topoisomerase, we further investigated whether they could perform similar inhibitory mechanisms on PARP1 (Staker et al., 2002). Topotecan mimics a DNA base pair and binds at the site of DNA cleavage by intercalating between the upstream (−1) and downstream (+1) base pairs (Topotecan, n.d.). Irinotecan prevents the religation of the DNA strand by binding to the topoisomerase I-DNA complex (Irinotecan, n.d.). Since the binding of both drugs occurs at the site of DNA, we docked the drugs onto a PARP-1 protein bound to a DNA double-strand break. The general docking of the original ligand, Topotecan, and Irinotecan are shown (Figure 4A). We continued our strategy of selecting amino acids within the 4 Angstroms limit for each specific docking (Figure 3B-D). The cost of energy for each molecule are -11.387 kcal/mol, -11.982 kcal/mol, and -11.387 kcal/mol respectively for the original ligand, Topotecan, and Irinotecan. The binding energies are generally slightly higher than the docking at the NAD+ site in Figure 3. The docking energy of Topotecan is again higher than that of the original ligand, whereas the docking energy of Irinotecan is identical. Taken together, structural and machine learning-based evidence all suggest that Topotecan might bind to and inhibit PARP1.

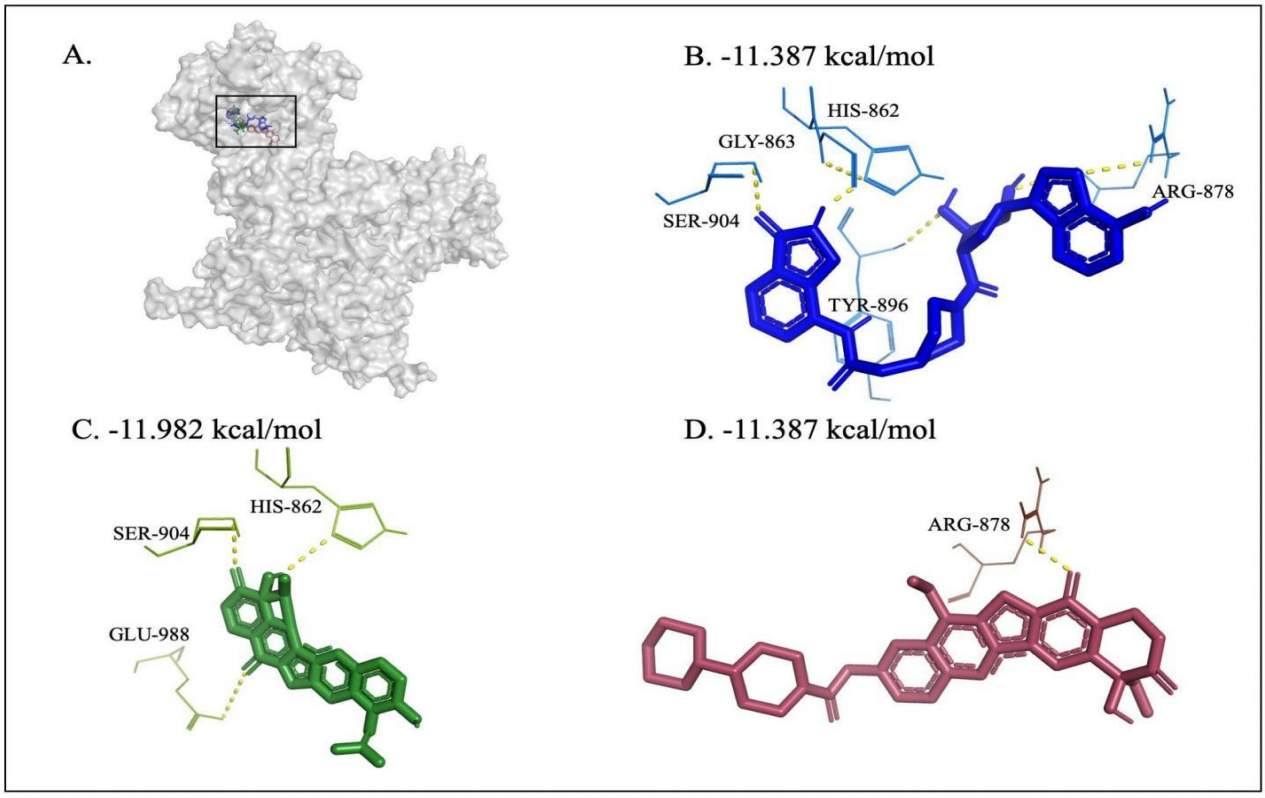

Figure 4. Binding conformations of the predicted PARP-1 inhibitors in PARP-1 protein bound to a DNA double-strand break.

A. Overall structure of PARP-1 (PDB ID: 7S6M), Topotecan, and Irinotecan at low magnification. The box represents the docked area. **B-D.** Docking of original ligand (B), Topotecan (C), and Irinotecan (D). The ligands are represented as sticks whereas the amino acids are represented as lines.

The polar contacts are in yellow dashed lines. The name of the original crystalised ligand is: 2-[4-[(2S,3S,4R,5R)-5-(6-aminopurin-9-yl)-3,4-bis(oxidanyl)oxolan-2-yl]carbonylpiperazin-1-yl]-N-(1-oxidanylidene-2,3-dihydroisoindol-4-yl)ethanamide.

3.4. Differential gene expression in the mouse brain upon topotecan treatment

In order to investigate the effect of topotecan treatment, we analyzed the gene expression of mice with breast cancer treated with topotecan (Pearson et al., 2016). We filtered the data by setting a limit of an adjusted P value lower than 0.001 and were left with 3428 genes. Then, we divided the data into two groups by the positivity of log fold change, separating genes that increased their number and those that decreased after the treatment (Figure 5A). After that, we put all genes in those groups separately into STRING, an online platform for Protein-Protein Interaction Networks Functional Enrichment Analysis (*STRING: Functional Protein Association Networks*, n.d.). The website returned different pathways in the protein-protein network. Among the many pathways, we focused solely on the UniProt pathway to investigate the function of genes in each group. The two functions with the highest strength in the increased and the decreased group were nucleotide biosynthesis (Figure 5B) and chromosomal rearrangement (Figure 5D) respectively. The result suggests that nucleotide biosynthesis was increased after the topotecan treatment whereas the chromosomal rearrangement was decreased.

The five genes that are associated with nucleotide biosynthesis are Prpsap1, Prpsap2, Prpas2, Dtymk, and Dctd. Phosphoribosyl pyrophosphate synthase-associated protein 1 (Prpsap1) and Phosphoribosyl pyrophosphate synthase-associated protein 2 (Prpsap2) are likely to play a negative regulatory role in 5-phosphoribose 1-diphosphate synthesis. Ribose-phosphate pyrophosphokinase 2 (Prpas2) belongs to the ribose-phosphate pyrophosphokinase family. It catalyzes the synthesis of phosphoribosylpyrophosphate (PRPP) which is essential for nucleotide synthesis. Deoxycytidylate deaminase (Dtymk) supplies the nucleotide substrate for thymidylate synthetase. Thymidylate kinase (Dctd) from the thymidylate kinase family catalyzes the conversion of dTMP to dTDP.

On the other hand, Satb1, Satb2, Braf, Trim24, and Tal1 are genes associated with chromosomal rearrangement. DNA-binding protein SATB1 is required for the switching of fetal globin species, and beta- and gamma-globin genes regulation during erythroid differentiation. It plays a role in chromatin organization and nuclear architecture during apoptosis. Satb1 is also a crucial silencing factor contributing to the initiation of X inactivation mediated by Xist RNA that occurs during embryogenesis and in lymphoma. DNA-binding protein SATB2 binds to DNA at nuclear matrix- or scaffold-associated regions. It is thought to recognize the sugar-phosphate structure of double-stranded DNA. Transcription factor controlling nuclear gene expression, by binding to matrix attachment regions (MARs) of DNA and inducing a local chromatin-loop remodeling. Satb2 acts as a docking site for several chromatin remodeling enzymes and also by recruiting corepressors (HDACs) or coactivators (HATs) directly to promoters and enhancers. B-raf proto-oncogene serine/threonine-protein kinase (Braf) is involved in the transduction of mitogenic signals from the cell membrane to the nucleus. It potentially plays a role in the postsynaptic responses of hippocampal neurons. Transcription intermediary factor 1-alpha (Trim24) is a transcriptional coactivator that interacts with numerous nuclear receptors and coactivators and modulates the transcription of target genes. It plays a role in the regulation of cell proliferation and apoptosis via its effects on p53/TP53 levels, and Up-regulates ligand-dependent transcription activation by AR, GCR/NR3C1, thyroid hormone receptor (TR), and ESR1. In addition, it modulates transcription activation by retinoic acid (RA) receptors and plays a role in regulating the retinoic acid-dependent proliferation of hepatocytes. It is required for the normal transition from proliferating neonatal hepatocytes to quiescent adult hepatocytes. Tal1, T-cell acute lymphocytic leukemia protein 1 homolog is implicated in the genesis of hemopoietic malignancies. It may play an important role in hemopoietic differentiation serving as a positive regulator of erythroid differentiation.

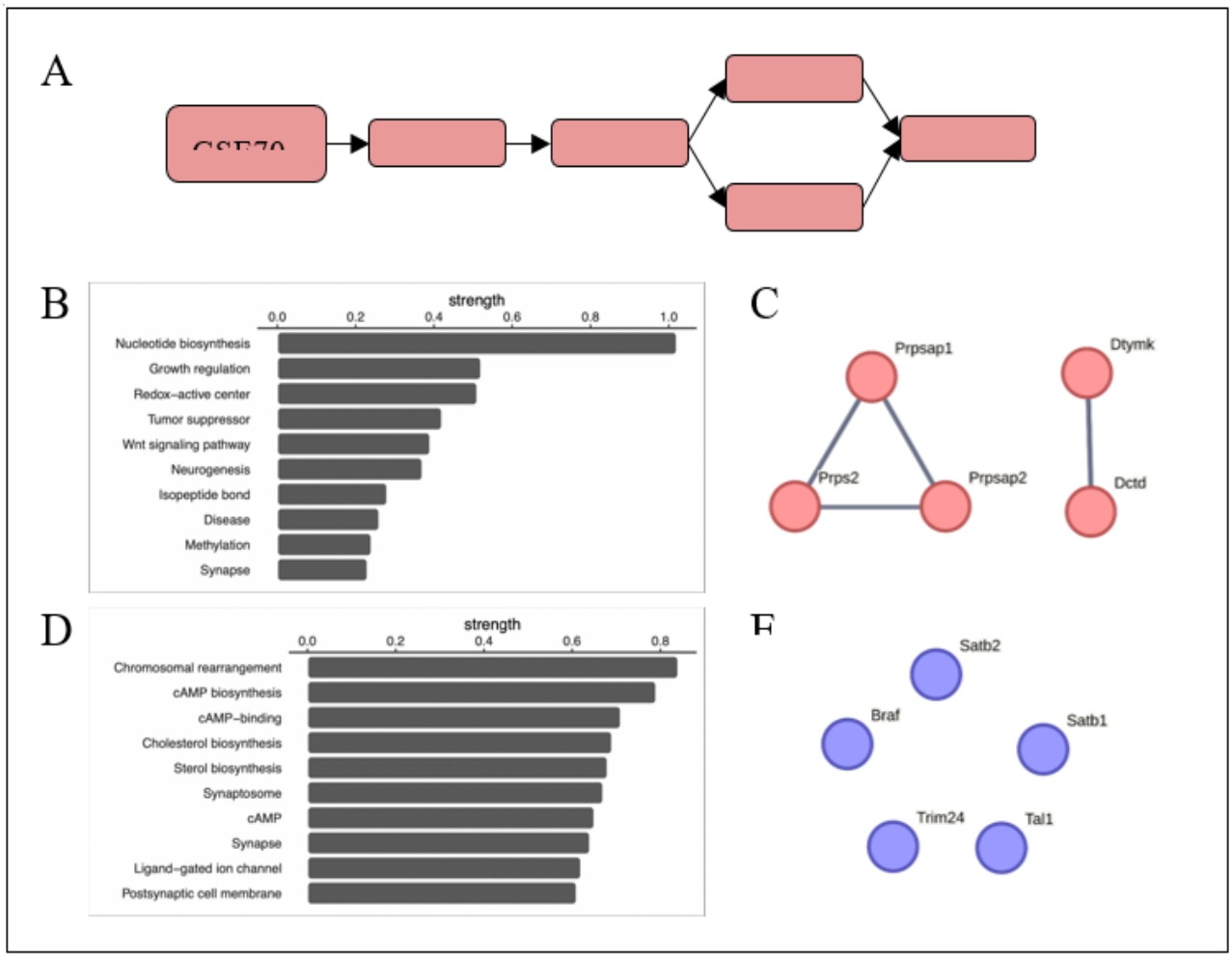

Figure 5. Increased nucleotide synthesis upon Topotecan treatment in the mouse brain.

Workflow of the RNA sequencing analysis pipeline. The first step is obtaining data and analyzing the gene expression and the second step is to investigate the increased and decreased gene and their functions. **B.** Significantly increased pathways. **C.** Genes involved in nucleotide binding. **D.** Significantly decreased pathways. **E.** Genes involved in the chromosomal rearrangement.

4. Discussion

PARP-1 overactivation is found in numerous chronic diseases including cancer and neurodegeneration (Rose et al., 2020, Yu et al., 2021). While successful PARP-1 inhibitors such as olaparib have been used clinically to treat cancer, they also have off-target effects that can be detrimental in subgroups of patients (Chen, 2011). This prompts the identification of novel PARP-1 inhibitors. Using known PARP-1 inhibitors, we trained a model to predict the IC50 value of drugs on PARP-1 protein. We found that Topotecan and Irinotecan, which are classically DNA topoisomerase inhibitors, might also inhibit PARP-1. To our knowledge, this information is novel and no previous study has investigated the effect of these 2 drugs on PARP-1.

The IC50 values predicted for these Topotecan and Irinotecan are 70 nM and 76 nM respectively. They are less efficient compared to olaparib, which has an IC50 of 5nM (Menear et al., 2008). However, we note that the predicted IC50 values have a high error rate, so the potential of Topotecan and Irinotecan to inhibit PARP-1 should be tested experimentally, along with olaparib as a positive control. Interestingly, the docking energy of Topotecan and Irinotecan align with the predicted IC50, in the sense that both the IC50 and the binding energy of Topotecan are lower than those of Irinotecan. This suggests that Topotecan might be a more potent PARP-1 inhibitor than Irinotecan.

Topotecan is a water-soluble analog of camptothecin, which was originally discovered in a search for anticancer drugs (Pratz et al., 2017). The activity of topotecan was also observed in non-small-cell lung cancer, refractory leukemias/myelodysplastic syndromes, and childhood sarcomas (Kollmannsberger et al., 1999). Topotecan has been shown to intercalate between topoisomerase-I and DNA, which traps topoisomerase-I.

Irinotecan is an antineoplastic enzyme inhibitor primarily used in the treatment of colorectal cancer and extensive small-cell lung cancer (along with cisplatin). Irinotecan prevents the religation of the DNA strand by binding to the topoisomerase I-DNA complex and causes double-strand DNA breakage and cell death (*Irinotecan*, n.d.). Irinotecan was approved for the treatment of advanced pancreatic cancer in October 2015 (irinotecan liposome injection, trade name Onivyde).

Both Topotecan and Irinotecan are inhibitors of topoisomerase I, an enzyme necessary for DNA replication (Pratz et al., 2017; Augustine et al., 2019). Topoisomerases (of both type I and type II) play a key role in the control of DNA topology. Cellular processes such as DNA replication, transcription, and recombination require physical access to the chromosomes' nucleotide bases. Topoisomerases change the topology of nuclear DNA and can "unwind" it, thereby making the nucleotides accessible. Inhibiting topoisomerase activity removes the cell's ability to change the topology of its DNA and thus blocks DNA synthesis and sister chromatid segregation (Węsierska-Gądek et al., 2012). The DNA topoisomerase thus becomes an excellent target for anticancer drugs due to these essential cellular functions.

Previous studies have found that PARP-1 could facilitate the religation activity of topoisomerase I by itself through topoisomerase I-PARP-1 interaction (PARP-1 action) or by the formation of poly(ADP-ribosyl)ation of topoisomerase I (PARP-1/NAD action) (Park & Cheng, 2005). Moreover, experiments also revealed that PARP-1 inhibition can increase the efficiency of anti-cancer drugs in cancer cells and suggest that mutations in other DNA repair proteins may render cancer cells more sensitive to interference with PARP-1 activity (Węsierska-Gądek et al., 2012).

We omitted Bryamycin in our molecular modeling analysis since the program that we used (Autodock Vina) is not suitable for predicting peptide-protein interactions. Bryamycin, also known as Thiostrepton, is a natural cyclic oligopeptide antibiotic of the ribosomally synthesized and post-translationally modified peptide class. Thiostrepton has been identified previously as an anticancer agent in a study of thiazole antibiotics and derivatives (Nicolaou et al., 2005).

To investigate the impact of Topotecan on gene expression, we analyzed RNA sequencing data from Pearson et al. (2016). We found that genes involved in synthesizing nucleotides are increased. Previous work by Yu et al., 2021 showed that inhibiting PARP led to an increase in the levels of nucleotide NAD+. Since the excessive PARP activation can cause the depletion of neurons of NAD, and contribute to mitochondrial dysfunction and cell death, an increase in nucleotide synthesis activity can increase the amount of NAD produced and thus slowing the progress of cell death, which might help to slow down the development of neurodegenerative diseases like AD. On the other hand, studies have shown that rapid instability is likely to affect PARP-1 cell growth and lead to the decline of PARP-1's proliferation (Lebel et al., 2003). A decreased activity in chromosomal rearrangement might as well contribute to a decrease in the proliferation of PARP.

While our analyses show that Topotecan and Irinotecan could inhibit PARP-1, they might not be the best drug candidates for AD therapeutic. Neurons are the cells that are primarily impaired in AD. These are post-mitotic or terminally differentiated, indicating that they do not perform cell division like cancerous cells. Inhibitors of cellular division like Topotecan and Irinotecan would thus have low toxicity for neurons. However, other brain cells like oligodendrocytes, astrocytes, and microglia are not post-mitotic and thus would require DNA topoisomerase for cell division. Inhibition of replication could lead to toxicity in those types of cells. In line with this, recent research showed that DNA topoisomerase inhibition could affect synaptic function (Mabb et al., 2014), suggesting caution in the use of this drug.

While our original goal was to develop PARP-1 inhibitors for AD treatment, we noted that the anticancer agents of Topotecan and Irinotecan might inhibit PARP-1 as well, uncovering an

additional target for these drugs. Since the inhibition of both PARP-1 and DNA topoisomerase could be beneficial in cancer, we reason that the anticancer potential of these drugs could be further explored.

References

[1] Anders, S., Heidelberg, E., & fs.tum.de >, ers at. (2016). *DESeq: Differential gene expression anal ysis based on the negative binomial distribution*. Bioconductor. https://www.bioconductor.org/packa ges//2.10/bioc/html/DESeq.html

[2] Antolin, A. A., Ameratunga, M., Banerji, U., Clarke, P. A., Workman, P., & Al-Lazikani, B. (2020). The kinase polypharmacology landscape of clinical PARP inhibitors. *Scientific Reports*, *10*(1). https://doi.org/10.1038/s41598-020-59074-4

[3] Antolín, A. A., & Mestres, J. (2014). Linking off-target kinase pharmacology to the differential cellular effects observed among PARP inhibitors. *Oncotarget*, *5*(10). https://doi.org/10.18632/oncotarget.1814

[4] Augustine, T., Maitra, R., Zhang, J., Nayak, J., & Goel, S. (2019). Sensitization of colorectal cancer to irinotecan therapy by PARP inhibitor rucaparib. *Investigational New Drugs*, *37*(5), 948–960. https://doi.org/10.1007/s10637-018-00717-9

[5] Benjamin, R. C., & Gill, D. M. (1980). Poly (ADP-ribose) synthesis in vitro programmed by damaged DNA. A comparison of DNA molecules containing different types of strand breaks. *Journal of* Biological *Chemistry*, 255(21), 10502–10508. https://doi.org/10.1016/s0021-9258(19)70491-8

[6] Chen, A. (2011). PARP inhibitors: its role in treatment of cancer. *Chinese Journal of Cancer*, *30*(7), 463–471. https://doi.org/10.5732/cjc.011.10111

[7] Dawson, T. M., & Dawson, V. L. (2017). Mitochondrial Mechanisms of Neuronal Cell Death: Potential Therapeutics. *Annual* Review *of Pharmacology and Toxicology*, *57*, 437–454. https://doi.org/10.1146/annurev-pharmtox-010716-105001

[8] Eberhardt, J., Santos-Martins, D., Tillack, A. F., & Forli, S. (2021). AutoDock Vina 1.2.0: New Docking Methods, Expanded Force Field, and Python Bindings. *Journal of Chemical Information and Modeling*. https://doi.org/10.1021/acs.jcim.1c00203

[9] Fatokun, A. A., Dawson, V. L., & Dawson, T. M. (2014). Parthanatos: mitochondrial-linked mechanisms and therapeutic opportunities. *British Journal of Pharmacology*, *171*(8), 2000–2016. https://doi.org/10.1111/bph.12416

[10] Franklin, H. (2018, August 8). *Advances in the use of PARP inhibitor therapy for breast cancer*. Drugs in Context. https://www.drugsincontext.com/advances-in-the-use-of-parp-inhibitor-therapy-for-breast-cancer/

[11] Hernández, F., Gómez de Barreda, E., Fuster-Matanzo, A., Lucas, J. J., & Avila, J. (2010). GSK3: a possible link between beta amyloid peptide and tau protein. *Experimental Neurology*, *223*(2), 322–325. https://doi.org/10.1016/j.expneurol.2009.09.011

[12] Hijazi, M., Smith, R., Rajeeve, V., Bessant, C., & Cutillas, P. R. (2020). Reconstructing kinase network topologies from phosphoproteomics data reveals cancer-associated rewiring. *Nature Biotechnology*, *38*(4), 493–502. https://doi.org/10.1038/s41587-019-0391-9

[13] Hou, Y., Dan, X., Babbar, M., Wei, Y., Hasselbalch, S. G., Croteau, D. L., & Bohr, V. A. (2019). Ageing as a risk factor for neurodegenerative disease. *Nature Reviews. Neurology*, *15*(10), 565–581. https://doi.org/10.1038/s41582-019-0244-7

[14] Houten, B. V., Hunter, S., & Meyer, J. (2016). Mitochondrial DNA damage induced autophagy cell death and disease. Frontiers *in Bioscience*, *21*(1), 42–54. https://doi.org/10.2741/4375

[15] Huber, C. M., Yee, C., May, T., Dhanala, A., & Mitchell, C. S. (2017). Cognitive Decline in Preclinical Alzheimer's disease: Amyloid-Beta versus Tauopathy. *Journal of Alzheimer's disease*, *61*(1), 265–281. https://doi.org/10.3233/jad-170490

[16] *Irinotecan*. (n.d.). Go.drugbank.com. https://go.drugbank.com/drugs/DB00762

[17] Jaeger, S., Fulle, S., & Turk, S. (2018). Mol2vec: Unsupervised Machine Learning Approach with Chemical Intuition. *Journal of Chemical Information and Modeling*, *58*(1), 27–35. https://doi.org/10.1021/acs.jcim.7b00616

[18] Kollmannsberger, C., Mross, K., Jakob, A., Kanz, L., & Bokemeyer, C. (1999). Topotecan – A Novel Topoisomerase I Inhibitor: Pharmacology and Clinical Experience. *Oncology*, *56*(1), 1–12. https://doi.org/10.1159/000011923

[19] Langston, J., Ballard, P., Tetrud, J., & Irwin, I. (1983). Chronic Parkinsonism in humans due to a product of meperidine-analog synthesis. *Science*, *219*(4587), 979–980. https://doi.org/10.1126/science.6823561

[20] Lebel, M., Lavoie, J., Gaudreault, I., Bronsard, M., & Drouin, R. (2003). Genetic Cooperation between the Werner Syndrome Protein and Poly (ADP-Ribose) Polymerase-1 in Preventing Chromatid Breaks, Complex Chromosomal Rearrangements, and Cancer in Mice. *The American Journal of Pathology*, *162*(5), 1559–1569. https://doi.org/10.1016/s0002-9440(10)64290-3

[21] Lee, Y., Karuppagounder, S. S., Shin, J.-H., Lee, Y.-I., Ko, H. S., Swing, D., Jiang, H., Kang, S.-U., Lee, B. D., Kang, H. C., Kim, D., Tessarollo, L., Dawson, V. L., & Dawson, T. M. (2013). Parthanatos mediates AIMP2-activated age-dependent dopaminergic neuronal loss. *Nature Neuroscience*, *16*(10), 1392–1400. https://doi.org/10.1038/nn.3500

[22] Lever, J., Krzywinski, M., & Altman, N. (2017). Principal component analysis. *Nature Methods*, *14*(7), 641–642. https://doi.org/10.1038/nmeth.4346

[23] Mabb, A. M., Kullmann, P. H. M., Twomey, M. A., Miriyala, J., Philpot, B. D., & Zylka, M. J. (2014). Topoisomerase 1 inhibition reversibly impairs synaptic function. *Proceedings of the National Academy of* Sciences, *111*(48), 17290–17295. https://doi.org/10.1073/pnas.1413204111

[24] Megino-Luque, C., Moiola, C. P., Molins-Escuder, C., López-Gil, C., Gil-Moreno, A., Matias-Guiu, X., Colas, E., & Eritja, N. (2020). Small-Molecule Inhibitors (SMIs) as an Effective Therapeutic Strategy for Endometrial Cancer. *Cancers*, *12*(10), 2751. https://doi.org/10.3390/cancers12102751

[25] Menear, K. A., Adcock, C., Boulter, R., Cockcroft, X., Copsey, L., Cranston, A., Dillon, K. J., Drzewiecki, J., Garman, S., Gomez, S., Javaid, H., Kerrigan, F., Knights, C., Lau, A., Loh, V. M., Matthews, I. T. W., Moore, S., O'Connor, M. J., Smith, G. C. M., & Martin, N. M. B. (2008). 4-[3-(4-cyclopropanecarbonylpiperazine-1-carbonyl)-4-fluorobenzyl]-2H-phthalazin-1-one: a novel bioavailable inhibitor of poly (ADP-ribose) polymerase-1. *Journal of Medicinal Chemistry*, *51*(20), 6581–6591. https://doi.org/10.1021/jm8001263

[26] Miller, M. B., Huang, A. Y., Kim, J., Zhou, Z., Kirkham, S. L., Maury, E. A., Ziegenfuss, J. S., Reed, H. C., Neil, J. E., Rento, L., Ryu, S. C., Ma, C. C., Luquette, L. J., Ames, H. M., Oakley, D. H., Frosch, M. P., Hyman, B. T., Lodato, M. A., Lee, E. A., & Walsh, C. A. (2022). Somatic genomic changes in single Alzheimer's disease neurons. *Nature*. https://doi.org/10.1038/s41586-022-04640-1

[27] Moriwaki, H., Tian, Y.-S., Kawashita, N., & Takagi, T. (2018). Mordred: a molecular descriptor calculator. *Journal of Cheminformatics*, *10*(1). https://doi.org/10.1186/s13321-018-0258-y

[28] Morshed, N., Lee, M. J., Rodriguez, F. H., Lauffenburger, D. A., Mastroeni, D., & White, F. M. (2021). Quantitative phosphoproteomics uncovers dysregulated kinase networks in Alzheimer's disease. *Nature* Aging, *1*(6), 550–565. https://doi.org/10.1038/s43587-021-00071-1

[29] Nicolaou, K. C., Zak, M., Rahimipour, S., Estrada, A. A., Lee, S. H., O'Brate, A., Giannakakou, P., & Ghadiri, M. R. (2005). Discovery of a Biologically Active Thiostrepton Fragment. *Journal of the American Chemical Society*, *127*(43), 15042–15044. https://doi.org/10.1021/ja0552803

[30] Park, S.-Y., & Cheng, Y.-C. (2005). Poly (ADP-Ribose) Polymerase-1 Could Facilitate the Religation of Topoisomerase I-linked DNA Inhibited by Camptothecin. *Cancer Research*, *65*(9), 3894–3902. https://doi.org/10.1158/0008-5472.can-04-4014

[31] Pearson, B. L., Simon, J. M., McCoy, E. S., Salazar, G., Fragola, G., & Zylka, M. J. (2016). Identification of chemicals that mimic transcriptional changes associated with autism, brain aging and neurodegeneration. *Nature Communications*, *7*(1). https://doi.org/10.1038/ncomms11173

[32] Pratz, K. W., Rudek, M. A., Gojo, I., Litzow, M. R., McDevitt, M. A., Ji, J., Karnitz, L. M., Herman, J. G., Kinders, R. J., Smith, B. D., Gore, S. D., Carraway, H. E., Showel, M. M., Gladstone, D. E., Levis, M. J., Tsai, H.-L., Rosner, G., Chen, A., Kaufmann, S. H., & Karp, J. E. (2017). A Phase I Study of Topotecan, Carboplatin and the PARP Inhibitor Veliparib in Acute Leukemias, Aggressive Myeloproliferative Neoplasms, and Chronic Myelomonocytic Leukemia. *Clinical Cancer Research: An Official Journal of the American Association for Cancer Research*, *23*(4), 899–907. https://doi.org/10.1158/1078-0432.CCR-16-1274

[33] *RDKit*. (n.d.). Www.rdkit.org. https://www.rdkit.org/

[34] Regier, M., Liang, J., Choi, A., Verma, K., Libien, J., & Hernández, A. I. (2019). Evidence for Decreased Nucleolar PARP-1 as an Early Marker of Cognitive Impairment. *Neural Plasticity*, *2019*, 1–8. https://doi.org/10.1155/2019/4383258

[35] Rose, M., Burgess, J. T., O'Byrne, K., Richard, D. J., & Bolderson, E. (2020). PARP Inhibitors: Clinical Relevance, Mechanisms of Action and Tumor Resistance. *Frontiers in Cell and Developmental Biology*, *8*. https://doi.org/10.3389/fcell.2020.564601

[36] Salech, F., Ponce, D. P., Paula-Lima, A. C., SanMartin, C. D., & Behrens, M. I. (2020). Nicotinamide, a Poly [ADP-Ribose] Polymerase 1 (PARP-1) Inhibitor, as an Adjunctive Therapy for the Treatment of Alzheimer's disease. *Frontiers in Aging Neuroscience*, *12*. https://doi.org/10.3389/fnagi.2020.00255

[37] *Saving a machine learning Model*. (2018, September 12). GeeksforGeeks. https://www.geeksforgeeks.org/saving-a-machine-learning-model/

[38] Speiser, J. L., Miller, M. E., Tooze, J., & Ip, E. (2019). A comparison of random forest variable selection methods for classification prediction modeling. *Expert Systems with Applications*, *134*, 93–101. https://doi.org/10.1016/j.eswa.2019.05.028

[39] Staker, B. L., Hjerrild, K., Feese, M. D., Behnke, C. A., Burgin, A. B., & Stewart, L. (2002). Nonlinear partial differential equations and applications: The mechanism of topoisomerase I poisoning by a camptothecin analog. *Proceedings of the National Academy of Sciences*, *99*(24), 15387–15392. https://doi.org/10.1073/pnas.242259599

[40] *STRING:* functional *protein association networks*. (n.d.). String-Db.org. Retrieved December 26, 2022, from https://string-db.org/cgi/input?sessionId=btmcFPIOe5cG&input_page_show_search=on

[41] *Topotecan*. (n.d.). Go.drugbank.com. https://go.drugbank.com/drugs/DB01030

[42] Wang, Y., Kim, N. S., Haince, J.-F. ., Kang, H. C., David, K. K., Andrabi, S. A., Poirier, G. G., Dawson, V. L., & Dawson, T. M. (2011). Poly (ADP-Ribose) (PAR) Binding to Apoptosis-Inducing Factor Is Critical for PAR Polymerase-1-Dependent Cell Death (Parthanatos). *Science Signaling*, *4*(167), ra20–ra20. https://doi.org/10.1126/scisignal.2000902

[43] Węsierska-Gądek, J., Zulehner, N., Ferk, F., Składanowski, A., Komina, O., & Maurer, M. (2012). PARP inhibition potentiates the cytotoxic activity of C-1305, a selective inhibitor of topoisomerase II, in human BRCA1-positive breast cancer cells. *Biochemical Pharmacology*, *84*(10), 1318–1331. https://doi.org/10.1016/j.bcp.2012.07.024

[44] Yu, Y., Fedele, G., Celardo, I., Loh, S. H. Y., & Martins, L. M. (2021). Parp mutations protect from mitochondrial toxicity in Alzheimer's disease. *Cell Death & Disease*, *12*(7), 1–10. https://doi.org/10.1038/s41419-021-03926-y

[45] Zhang, M., Holowko, M. B., Hayman Zumpe, H., & Ong, C. S. (2022). Machine Learning Guided Batched Design of a Bacterial Ribosome Binding Site. *ACS Synthetic Biology*, *11*(7), 2314–2326. https://doi.org/10.1021/acssynbio.2c00015